Title
Feedback System Control in Combinatorial Nanodiamond-based Drugs Optimization in vitro in Breast Cancer

Author
Chen, Kai-Yu

Publication Date
2015

Peer reviewed|Thesis/dissertation

UNIVERSITY OF CALIFORNIA

Los Angeles

Feedback System Control in Combinatorial Nanodiamond-based Drugs Optimization *in vitro* in Breast Cancer

A thesis submitted in partial satisfaction

of the requirements for the degree Master of Science

in Bioengineering

by

Kai-Yu Chen

2015

ABSTRACT OF THE THESIS

Feedback System Control in Combinatorial Nanodiamond-based Drugs Optimization *in vitro* in Breast Cancer

by

Kai-Yu Chen

Master of Science in Bioengineering

University of California, Los Angeles, 2015

Professor Dean Ho, Chair

Combinatorial drugs have been used for decades to improve therapeutic efficacy in cancer treatments through drug synergistic mediation. Although they are believed to have good efficiency in killing cancer cells by simultaneously suppress multi-drug resistances through targeting different cellular mechanisms, its remedial effects is still limited when considering heterogeneity of cancer cells. Recently, nanosystem-based agents have become new drug delivery systems to improve therapeutic efficiency as well as safeness. However, it is still difficult to optimize desired therapeutic combinations and fails to enhance drug efficacy efficiently. Thus, feedback system control (FSC) platform has been introduced to circumvent limitations in optimizing drug combinations for either unmodified or nanotechnology driven therapeutics. The FSC platform provides an algorithm that integrally and swiftly produces an ideal combination consisting of three nanodiamond-modified anticancer drugs: doxorubicin,

mitoxantrone, bleomycin and one unmodified anticancer drug- paclitaxel. Particularly, the therapeutic windows obtained from the FSC-based nanodiamond-drug combinations were significantly higher than the ones in optimized unmodified drug combinations, single nanodiamond and unmodified drug administration, and randomly sampled nanodiamond-drug combination treatment. Moreover, the FSC methodology intrinsically considers cancer cell heterogeneity and sophisticated intracellular mechanisms. This approach can be potentially applied in optimizing multi-therapeutic systems clinically, expressing a favorable candidate in personalized medication development in the future.

The thesis of Kai-Yu Chen is approved.

Daniel Kamei

Pei-Yu Chiou

Dean Ho, Committee Chair

University of California, Los Angeles

2015

TABLE OF CONTENTS

ACKNOWLEDGEMENT

First, I would like to express my sincere thanks to my advisor, Professor Dean Ho, for the endless support of my master research, for his motivation, patience, and great knowledge. I appreciate he gave me a chance cooperating with Professor Chih-Ming Ho and his research team in the FSC project, which broadened my horizon in modeling and new applications in cancer treatment. His guidance helped me in the research and writing of this thesis. I am sincerely thankful that I have such a great advisor during my master's research. His ambitions and passions greatly enlighten my interests and enthusiasm in research again.

I would also like to thank the rest of my thesis committee: Professor Daniel Kamei and Professor Pei-Yu Chiou, for their guidance and help in the completion of my master thesis.

In addition, I sincerely thanks to my dear senior lab mates and mentors, Hann Wang, Dong-Keun Lee, and Kangyi Zhang, who were like my big brothers and provided me with many suggestions in the research as well as helped me to familiarized the laboratory and research facilities. Especially, in this project, the both postdoctoral researchers, Hann Wang, and Dong-Keun Lee lead the whole project. Hann Wang who contributed greatly in machine settings and data analysis. He kindly taught me about the modeling and data analysis, which greatly stimulated my interests in simulation and statistics. In this project, Dong-Keun Lee did all the synthesis and modifications of ND-drugs. He also took care of machine operation and data analysis. He inspired me with the passion and the importance of perseverance in research. I would also like to express my thanks to Jing-Yao Chen for assisting in some cell cultures and Kangyi Zhang, Aleidy Silva for helping writings and suggestions. I sincerely appreciate Professor Dean Ho and

Professor Chih-Ming Ho in guiding and managing this project. Without their precious support, it would not be possible to conduct this research.

I appreciate my fellow lab mates for the time we spent together in the lab, and for all the fun we have had in the last two years. Also, I thank my awesome friends at UCLA who gave me unforgettable fun lives in LA. In particular, I am grateful to Bingling Wang, Jett Lee, Alex Lee, Yawen Cheng, I-Fan Shih, Willy Ching, Bruce Chen, Hui-Yin Shiu, Patrick Jou for endless support and great times during my master study.

Finally, I would like to honestly thank my parents, aunts, cousins, and Dr. Gibert Bane for supporting me spiritually throughout writing this thesis and my graduate life in general.

Feedback System Control in Combinatorial Nanodiamond-based Drugs Optimization *in vitro* Breast Cancer

Published in

Hann Wang, Dong-Keun Lee, Kai-Yu Chen, Jing-Yao Chen, Kangyi Zhang, Aleidy Silva, Chih-Ming Ho*, and Dean Ho*.

"Mechanism-Independent Optimization of Combinatorial Nanodiamond and Unmodified Drug Delivery Using a Phenotypically Driven Platform Technology"

ACS Nano, 2015, 9 (3), pp 3332–3344, DOI: 10.1021/acsnano.5b00638

1. Introduction

1.1 Drug Resistance caused Limitation in Cancer Therapy

Single-drug chemotherapy targeting specific intracellular signaling pathway that stimulates cancer development have shown to be effective in several cases of tumors in many previous researches. Even though their continuous improvement in inhibition of cell proliferation, glycolysis, angiogenesis, and other key biomarker in tumors, challenges in patient toxicity, drug resistance, and therapeutic efficacy remain to be solved[1]. The resistance of tumor cells results from inherent properties of the complex intracellular mechanisms. Some studies have shown that such complex networks contribute to the dynamics and variations of tumor cells. Inherent and acquired multiple-drug resistance is one of the results from complex cellular networks characterized by alternative pathways, robustness, and compensatory ability. These interwinded networks enable tumor cells detect and efflux chemotherapeutic agents as well as immediately evolve against drug toxicity. These scenarios often result in limited remedial effects [2-4]. Many patients face tragic recurrence at last. Thereby, to solve these problems, it is crucial to simultaneously address several remedies in cancerous cellular networks with an agent or system.

1.2 Doxorubicin, Bleomycin, Mitoxantrone, and Paclitaxel in Cancer Treatment

Doxorubicin is an anticancer drug commonly used in chemotherapy and belongs to the anthracycline-related compound. DNA replication requires relaxation of supercoils by topoisomerase Ⅱ during the DNA transcription process. Doxorubicin intercalates into DNA helix and inhibits the activity of the topoisomerase Ⅱ by stabilizing the complex. This process further prevents the DNA double helix from being resealed and thereby terminating the replication

procedures [5,6]. Doxorubicin is also often used in combination chemotherapy regimen[7,8]. However, its component of anthracycline leads to cardiotoxicity, which is a major limitation in clinical applications. Formation of free oxygen radicals, disruption of the mitochondrial metabolism and overloading of intracellular calcium are considered as the pathological mechanisms. In other words, the main downside of doxorubicin used in cancer chemotherapy is being toxic and causes cardiomyopathy, hence induced congestive heart failure[9].

Bleomycin is also one of the drugs that typically used in cancer chemotherapy. The actual mechanism of bleomycin interaction of DNA is yet to be solved. Some researchers suggested that bleomycin induces the breakage of DNA strands by its bithiazole structure and by pyrimidine- and imidazole-structurally binding to ions or oxygen. This process forms an oxidant and leads to strand scissions, thus stops DNA replications. However, such process may cause interstitial pneumonia followed by pulmonary fibrosis and impair lung functions[10].

Mitoxantrone is also an anthracenedione agent and is often used in treating many types of cancer, including metastatic breast cancer and myeloid leukemia. Mitoxantrone is structurally related to doxorubicin. It also intercalates into DNA strands and inhibits topoisomerase Π, thereby ceases DNA repair- and DNA synthesis systems. It has been associated with the progress of left ventricular impairment. Cumulative mitoxantrone dosage is deemed as an indication of a higher risk of damage in cardiac cells. Yet, some studies have shown that mitoxantrone is well tolerated and provides remarkable therapeutic efficiency and less toxic than the current single drugs. These properties makes it become one of the component in the combination regimens to treat breast cancer and other types of cancer[11,12].

Paclitaxel serves as the taxane family of anticancer drugs. Unlike anticancer drugs mentioned previously, which disturb proliferation of cancer cells by breakage of DNA strands or interfering replication process, paclitaxel malfunctions microtubules. Microtubules are regarded as bones of cells and will be rearranged during cell division. However, these microtubules will be very stable and lose their functions in the presence of paclitaxel. Paclitaxel promotes the polymerization of tubulin and interferes with the interphase process of mitosis. This abnormal cellular process disrupts cell division and eventually leads to apoptosis. In addition, Paclitaxel is increasingly used in combination therapies with doxorubicin in advanced breast cancer and ovarian cancer [13].

1.3 Combinatorial Drugs Therapy in Cancers

In order to overcome the challenges faced by drug resistance, combinatorial drugs have been introduced. Combinatorial therapy has been regarded as a major advance in current clinical cancer treatment. Combinatorial therapy is an agent that consists of various drugs with different anti-cancer mechanisms operating simultaneously in combating heterogeneity and dynamics of tumors. Such therapeutic agents may enhance adjustment in the cellular systemic network, reduce the probability of recurrence and demonstrate higher selectivity against cancer cells over healthy cells [14-16]. Combinatorial chemotherapeutic agents have been adopted as a common standard of care against many types of cancer, such as melanoma, colon rectal, and pancreatic cancers[17-19]. They have proven to be more efficient than sequential single drug treatment at preventing drug resistance [20]. However, traditional combination therapies are often additively or scaling- determined in preclinical tests. Moreover, maximum tolerated dose (MTD) was adopted by the previous combinatorial drug regimens, which was believed to be efficient in killing cancer

cells. Yet some studies have proven that using MTD cannot always guarantee highly therapeutic efficacy[21]. Although combinatorial therapeutic treatments seem promising in clinical applications, they are difficult to optimize dosages in combination therapies when considering the heterogeneity of patients and types of tumors.

Traditional methods to improve the therapeutic effects of combinatorial drugs have relied upon linear additive synergism and antagonism. Currently scientists have found non-linearity strategies in examining interaction between drugs[22-24]. However, these strategies have yet to utilize successfully a systemic platform that can develop the connection between input signal and output response at the same time. To solve this limitation, the feedback system control (FSC) platform has been introduced to optimize combinatorial drug design. This FSC platform has the ability to generate a drug-dose response quadratic surface without repeatedly feedback search and screen[25]. It also creates a therapeutic window surface rapidly based on experimental results and promptly identifies the optimal drug combinations that provide greater safety and efficacy.

1.4 Nanodiamond Drugs and the Feedback System Control

In addition to manipulating drug combinations for cancer therapy, modifying the drug itself could be another strategy to improve therapeutic efficiency and lower drug toxicity. Currently, many researches have pointed out that drugs carried by nanoparticles, such as micelles, polymersomes, and nanodiamonds (NDs), may significantly reduce drug toxicity as well as drug resistance, therefore increase drug circulatory half-time and permeability in tumors[26-28]. As a result, combining multiple drugs onto the surface of nanoparticles may further dramatically boost

therapeutic effects in cancer treatments. In this thesis, NDs were applied as a drug delivery agent due to their unique characteristics in electronics, chemistry, and biology in comparison with other nanomedicine systems. NDs can also be harnessed to bind to extensive kinds of tiny compounds and form ND-drugs. These tiny compounds could be well distributed on the surface of the NDs owing to their exclusive facet-based electrostatic natures. Drugs adhered to the surface of NDs can be release without chemical modification. In addition, NDs are biocompatible and are well tolerated in cells, thus they have sustained intracellular retention time. Given these advantages, ND-drugs can be characterized by enhanced therapeutic efficacy and diminished cellular toxicity[29-32]. It should be noted that ND-drugs have remarkably increased the remedial safety and efficiency of the cancerous therapeutics in many preclinical studies.

With the outstanding performance in the FSC platform and the unique natures that NDs possess, it is reasonable to believe that an association of such a platform with combinatorial ND-drugs could be regarded as a promising solution in chemotherapy (Figure 1). The combinatorial drug composed ND-doxorubicin (ND-DOX), ND-bleomycin (ND-BLEO), ND-mitoxantrone (ND-MTX), and paclitaxel (PAC). The use of the FSC methodology in optimizing the combination of ND-drugs can be achieved in three steps (Figure 2). The first step focused on determining the concentrations of the four drugs. Latin hypercube sampling was used to cover a broad range of dosage domain and to create various drug combinations, which thereby built a response surface. In the second step, the therapeutic window surface was built by experimental screening of the cellular viability. The safety and efficiency of these drug combinations created by Latin hypercube sampling were estimated by conducting the viability assays in three control cell lines (MCF10A, H9C2, and IMR-90) and in three breast cancer cell lines (MDA-MB-231,

BT20, MCF7) with distinct resistance to anticancer drugs. In the final step, regression analysis was used to verify the availability of the model built by the FSC platform followed by utilizing the differential evolution approach to derive global optimization in the concentrations of the combinatorial drug regimen.

Based on the study, the therapeutic efficacy of the FSC-optimized drug combinations were exceeded the one in both ND-modified and unmodified single drug administration, combinatorial unmodified drugs, and randomly formulated drug combinations. Instead of considering all of the complex cellular signaling pathways for the complicated modeling prediction and the theoretical assumption, the incorporation of the FSC platform with NDs wisely reconciled cellular phenotypic response to therapeutic uncertainty by experimental validation. Therefore, the FSC platform serves as an effective and efficient method toward combinatorial drug development in treatments of cancers and other diseases.

2. Materials and Methods

2.1 Cell Culture

The three breast cancer cell lines were: (1) MDA-MB-231, human breast adenocarcinoma cells; (2) MCF7, human breast carcinoma cells; (3) BT20, human breast carcinoma cells. The three control cell lines were: (4) MCF10A, human breast epithelial cells; (5) IMR-90, human lung fibroblast cells, (6) H9C2 (rat myocardium myoblast cells. They were obtained from American Type Culture Collection (ATCC). The MDA-MB-231 cells were cultured in a high glucose RPMI-1640 medium containing HEPES and l-glutamine (ATCC), added with 10 % FBS (GEMINI). The H9C2 cells, IMR-90 cells, BT20 cells, and MCF7 cells were cultured in DMEM containing 4.5 g/l D-glucose and l-glutamine, included 10% FBS. The MCF10A cells were maintained in a DMEM/F12 medium containing 15mM HEPES and l-glutamine supplemented with 5% horse serum (GIBCO), along with, 0.1% epithelial growth factor, 0.1% hydrocortisone, and 0.1% insulin from MEGM SingleQuot Kit (ATCC). When 70-80% confluence was reached, subculturing was performed at a ratio of 1:4. A solution of 0.25% of the Trypsin-EDTA (GIBCO) was applied to the MCF10A, human epithelial breast cell line, while 0.05% Trypsin-EDTA (GIBCO) was applied to the other five cell lines to detach the cells from the cell flask.

2.2 Cell Plating

All cell lines were detached using trypsin-EDTA. After centrifuging at a speed of 1000 rpm for five minutes, cell pellets were pipetted gently and cells were counted using a hemocytometer (HAUSSER SCIENTIFIC). A Biomek FX^p robot (Beckman Coulter) was used to seed the cells

onto 96-well plates with a density of 10000 cells per 75 μl. The outer rows and columns of each 96-well plate were excluded because those wells tend to have higher evaporation rates. These wells can cause a large standard deviation in the experimental results.

2.3 Single-Drug Testing

The unmodified and ND-modified doxorubicin, mitoxantrone, bleomycin, and unmodified paclitaxel were applied onto a 96-well plate through serial dilution after cell plating. The drugs were loaded into corresponding wells with the Biomek FX^p robot in triplicate version.

2.4 Combinatorial-Drug Testing

After serial dilution, these drugs were applied onto a 48-well plate. The initial concentration of each drug was determined based on the individual result of single-drug testing. Latin hypercube sampling was used to determine drug combinations and these drug solutions were plated onto a 96-well plate. They were transferred onto the corresponding wells on a 96-well cell plate. Cells with applied drug solutions were incubated at 37°C for 72 hours.

2.5 Cell Viability Assays

Cell viability was tested after 72 hours of incubation in the drug solution; 0.5 mM resazurin (Sigma) was applied to the 96-well cell plates. After incubation of 3 hours at 37°C and 5% CO_2, cell viability was then obtained from fluorescent readings at 560 nm/590 nm.

The viability function is composed of two variables – a disease-causing mechanism, d, and the

drug concentration, c. The viability function in a diseased profile under the drug treatment can be expressed as V(d,c), while the diseased biological system before the treatment is written as V(s,0). Recalled the mathematical Taylor expansion, the higher order term can be neglected since their values are much smaller than the first and second order term[33,34]. Therefore, the therapeutic efficacy of the combinatorial drug can be represented by

$$V(d,c) - V(d,0) \approx \sum_k a_k c_k + \sum_i b_i c_i^2 + \sum_m \sum_n D_{mn} c_m c_n$$

The third term on the right side of the equation represents the interaction between the drugs. When these drugs demonstrate synergistic interaction, it can be expressed as $\sum_m \sum_n D_{mn} c_m c_n > 0$, whereas the term would become negative if there are antagonistic effects. Although the functions of a diseased profile after the treatment V(d,c) and before the treatment V(d,0), were unknown, the therapeutic efficacy could be studied. It should be noted that the exact complex biological mechanism does not need to be investigated with this equation. The coefficients of this algebra series were derived from tests in different concentration combinations.

2.6 Synthesis of the Nanodiamond Drugs

Doxorubicin hydrochloride, mitoxantrone dihydrochloride (Sigma-Aldrich), bleomycin sulfate (Cayman Chemical, Ann Arbor, MI, USA), and NDs (Nagano, Japan) are used to synthesize ND-drugs. First, each drug was mixed with deionized sterilized water at a concentration of 5mg/ml. Doxorubicin and mitoxantrone were mixed with autoclaved NDs at a ratio of 5:1 (w/w), with bleomycin of 5:2 (w/w). 2.5 mM NaOH was then added to ionize drugs and incubated for 96 hours at room temperature (RT), enabled them attach to the surface of NDs. The ND-drug.

The final ND-drug solutions with concentrations of 5 mg/ml were made by resuspending them with deionized water after being centrifuged down and washed with deionized water until transparent.

2.7 Characterization of the Nanodiamond Drugs

To determine loading efficiency, unbound drugs in the supernatant were analyzed. The supernatant containing free doxorubicin, mitoxantrone, and bleomycin were measured at an absorbance of 550, 590, and 290 nm. The concentration of drugs coupled on the surface of the nanodiamond was determined by a standard curve derived from the absorbance of serial dilutions of the drug, ranging from 0 to 200 μg/ml.

To assure the presence of drugs on the surface of the NDs, 2 mg of ND, drugs, and ND-drugs were mixed with 100 mg of potassium bromide using mortar and pestle. These samples were pelletized to make a thin disc for FTIR spectroscopy analysis with a resolution of 1 cm^{-1} and 64 scan accumulations. A Zetasizer Nano ZS (Malvern Instrument, UK) was used to measure the size and zeta potential of nanodiamonds and ND-drugs. Sizes of ND-drugs were measured at a 173° backscattering angle with three runs at 25°C. The zeta potential was obtained at 25°C in water by clear zeta cells (DTS-1060C). The hydrodynamic diameter was also obtained from the z-average values from the three runs.

2.8 Sampling of Drug Dosage and Drug Combination Optimization

Latin hypercube was processed in the sample space Ω, where the input $Y \in \Omega Y$; with the

sample be Yij, i = 1,..., M and j = 1,..., N. M represents the number of strata, whereas N represents the number of drug categories. The range of Yj was divided into M strata, and a component from each stratum was determined. Prior to Latin hypercube sampling, the dosage range of each unmodified and ND-modified doxorubicin, mitoxantrone, bleomycin, and unmodified paclitaxel anticancer drug were decided based on the result of single-drug testing. The range was decided from the concentration of zero fatal effects to the concentration of maximum fatal effects for cancer cell lines. The concentration of the drug was determined according to the cell viability measurements. The log concentration was then applied in each drug and divided into seven strata within the drug dosage range followed by Latin hypercube sampling.

To maximize combinatorial drug therapeutic efficacy in fighting against cancer cells while minimizing drug toxicity in control cells, that is, to maximize the value of the therapeutic window - the difference between viability in the control cell line and the cancer cell line. The differential evolution approach was used to identify the optimal drug combinations on the therapeutic response surface generated from the central composite design.

2.9 Verification and Prediction by Statistical Analysis

The FSC-optimized ND-drug combinations were compared with the group of the modified and unmodified single drug administration, unmodified drug combinations, and randomly sampled modified ND-drug combinations with a student t-test statistical analysis. A p-value of less than 0.05 represents a statistical significance. Pearson correlation analysis was conducted to see the

correlations between the FSC-predicted values and experimental values. A t-test is held based on the hypothesis that the experimental therapeutic window was derived from a normal distribution with a predicted mean and an unknown variance was investigated for the response surface construction.

3. Results

3.1 The Cellular Response Surface and the Optimal Therapeutic Windows of the FSC-based ND-Drug Combinations

Feedback system control is believed to accurately and rapidly predicts the optimal therapeutic window in optimal ND-drug combinations. The formation of a therapeutic window was created based on the cellular response surface from the application of a set of four drugs on six cell lines. To determine the range of each drug in each cell line, a dose-response curve was created in the set of four drugs by conducting a nine-stage, 2.5 serial dilution in the six cell lines. The range of each drug concentration in each cell line lies between the maximum lethal concentration and the zero lethal concentration (cell viability >95%). The final concentration range for each drug had to cover the concentration ranges of all the cell lines and was divided into seven dilution stages with specific folds. In the FSC-optimized ND-drug combination, the maximum concentration of ND-DOX, ND-BLEO, ND-MTX, and PAC was 9.0×10^{-5} M, 2.0×10^{-6} M, 1.3×10^{-4} M, and 2.0×10^{-5} M, coupled with a fold of 4.5, 4.47, 6.18, and 6.8, respectively (Table 1).

A total of 57 drug combinations that consisted of different four drug concentrations (shown by different stages) were derived from Latin hypercube sampling (Table 2). To show this five-dimensional response surfaces in three dimensions, two of the drug concentrations were fixed at optimal dosage as constants. The cellular response surface was plotted according to the trend of the concentration of the other two drugs on the cell viability (Figure 3 A,B,D,E,G,H). A response surface of therapeutic window was built upon the difference of cell viability from one type of cancer cell line and one type of control cell line in the two varying concentrations of the

drug, holding the other two concentrations of the drug constant (Figure 3 C, F, I).

The goal of the feedback system control is to derive a drug combination that maximizes a therapeutic window value. Differential evolution approach was used to achieve the global optimal dosage from the therapeutic windows graphs. This dosage eliminated the maximum numbers of cancer cells while maintaining the maximum numbers of control cells to maximize the value of the therapeutic windows. In the case of MCF10A and MDA-MB-231 cell lines (Figure 3C), the experimental optimal therapeutic window was 51.50±3.51%, with a blue pyramid represents the experimental mean and the height of the pyramid represents the experimental standard error. The optimal dosages in the ND-drug combinations were 9.88×10^{-7} M, 2.10×10^{-5} M, 1.12×10^{-9} M, 2.02×10^{-10} M in ND-DOX, ND-MTX, ND-BLEO, and PAC, accordingly. The optimal therapeutic window value predicted by the FSC platform was 47.01% given the same dosages. A t-test was done to verify the significant difference between the predicted values and the experimental results. The null hypothesis would not be rejected if a p-value was greater than 0.05. That is, the predicted values match to the experimental results. In this case, the p-value was 0.35, indicating that there was no significant difference between the predicted optimal therapeutic window values generated by the FSC platform and the experimental one.

In the group of the H9C2 and MDA-MB-231 cell lines (Figure 3F), the experimental optimal therapeutic window was 21.46±4.0%. The optimal dosages in ND-drug combination were 4.88×10^{-8} M, 2.34×10^{-9} M, 2.0×10^{-6} M, and 2.0×10^{-5} M in ND-DOX, ND-MTX, ND-BLEO, and PAC. The optimal therapeutic window value predicted by the FSC platform at the same

concentrations was 20.71%. The p-value was 0.78, suggesting that there was a significant statistical connection between the FSC-predicted optimal value and the experimental optimal value.

On the therapeutic window surface of the IMR-90 and MDA-MB-231 cell lines (Figure 3I), the experimental optimal therapeutic window was 15.80±6.19%. The optimal dosages for ND-drug combination were 1.08×10^{-8} M, 8.93×10^{-8} M, 4.47×10^{-7} M, 2.94×10^{-5} M in ND-DOX, ND-MTX, ND-BLEO, and PAC, respectively. The optimal therapeutic window forecast by the FSC methodology was 9.53% at the same drug concentrations, with a p-value of 0.48. The FSC-predicted value was close to the experimental therapeutic window value.

3.2 Verification of Experimental Measurement and Model Prediction

To valuate the preciseness of the model, the FSC predictions were compared to experimental results through Pearson correlations (Figure 4). As a result, The Pearson correlation coefficients were 0.9, 0.93, 0.93, 0.93, 0.82, and 0.92 in the case of MCF10A, H9C2, IMR-90, MDA-MB-231, MCF7, and BT20 cell lines, respectively. The high value of the Pearson correlation coefficients represents high linear relationships between predicted values and experimental results[35], indicating that the FSC can provide a precise and efficient prediction for the experimental optimal value. Based on the results, it is concluded the FSC platform can successfully and strongly select the ideal ND-drug combination as well as predict the optimal therapeutic windows.

3.3 The Therapeutic Windows of Single Drug Administration

Each single drug DOX, MTX, BLEO, ND-DOX, ND-MTX, ND-BLEO, PAC was serially diluted and administered to each of the six cell lines MCF10A, H9C2, IMR-90, MDA-MB-231, MCF7, BT20 to experimentally derive the optimal dosage and the maximum therapeutic window. The optimal therapeutic window of the single drug administration was 30.22±10.62% via ND-BLEO administration.

3.4 The Optimal Therapeutic Windows of Unmodified-Drug Combinations

Similar to ND-drug combinations, Latin hypercube sampling was used to select 57 combinations from a set of four unmodified drugs: doxorubicin, mitoxantrone, bleomycin, and paclitaxel. These combinations were applied onto three control cell plates of the MCF10A, H9C2, IMR-90 cell line and one cancer cell line, the MDA-MB-231. The differential evolution method was addressed to derive the optimal combination from the therapeutic window surface. The optimal therapeutic windows in the case of MCF10A−MDA-MB-231, H9C2−MDA-MB-231, and IMR0-90−MDA-MB-231 were 31.10±2.50%, 4.94±5.06%, and 2.20±3.66%, respectively.

3.5 The Therapeutic Windows of Randomly Sampled ND-Drug Combinations

Again, the 57 drug combinations were randomly sampled through Latin hypercube sampling and applied into the six cell lines. Differently, in the group of randomly sampled ND-drug combinations, the therapeutic windows from each of the 57-drug combinations were averaged to compare the results from the optimal therapeutic windows derived from the FSC. The average values of these therapeutic windows are shown in Table 3. Among the nine therapeutic windows,

only two of the cases showed positive values, while the remaining seven cases had negative values. The average therapeutic windows for the pair of H9C2−BT20, H9C2−MCF7, H9C2−MDA-Mb-231, IMR-90−BT20, IMR-90−MCF7, IMR-90−MDA-MB-231, MCF10A−BT20, MCF10A−MCF7, and MCF10A−MDA-MB-231 were 0.03, -0.20, -0.02, 0.02, -0.21, -0.04, -0.05, -0.29, -0.11. These results indicated that the randomly sampled ND-drug combinations barely found good therapeutic windows and thus this method could be limited to produce the optimal drug combinations.

3.6 ND-drug synthesis and characterization

Fourier transform infrared spectroscopy (FTIR) spectra were used to confirm the coupling of DOX, MTX, and BLEO with NDs by comparing their peaks (Figure 9A). Peaks at 780-850, 1560-1590, 1603-1616, and 1620-1650 cm^{-1} can be observed from the ND-drug and were absent in the NDs only. These peaks indicated the C=C-H bending vibrations, with two peaks representing C=C and C=O stretching vibrations. ND-drugs had broad stretching vibrations of C=O formed on the ND surfaces in the spectral region of 1700 to 1800 cm^{-1}. Moreover, unmodified drug and ND-drugs showed similar vibrational spectra profiles and the same vibrations in specific bands due to certain functional groups.

Dynamic light scattering was used to compare and analyze the sizes of the NDs and the ND-drugs (Figure 9B). All the samples were measured in the water environment and the sizes were represented by hydrodynamic diameters. The average size of NDs was 46.60±17 nm, whereas the average sizes of the ND-DOX, ND-MTX, and ND-BLEO were 120.0±0.93,

109.2±0.58, and 105.1±0.53 nm, indicating successfully coupling of the NDs with drugs. In addition, the ζ-potential of NDs was 55.8±0.37 mV, while the ζ-potentials of ND-DOX, ND-MTX, and ND-BLEO were shrunk to 45.3±0.51, 47.8±0.66, and 52.0±0.35 mV. It should be noted that good homogeneity of nanomedicine is regarded as a crucial property in drug delivery platform. These results demonstrated that both NDs and ND-drugs have shown a narrow distribution range and similar ζ-potentials, indicating of excellent homogeneity[36,37].

UV spectroscopy was used to acquire the quantity of drugs coupled with NDs by reading the absorbance of the supernatants (Figure 9C). The DOX, MTX, and BLEO were measured at 550 nm, 590 nm, and 290 nm, respectively. As a result, the loading efficiencies of DOX, ND-MTX, and ND-BLEO were 876 ±2.8, 987±1.0, and 329±1.0 μg.

4. Discussion

4.1 Unmodified and ND-modified drugs

Combining four different kinds of anticancer drugs was considered to be mechanism-compensated in increasing drug efficacy. Doxorubicin, mitoxantrone, and bleomycin were selected due to their immediate ability to bind to nanodiamonds. Unmodified paclitaxel was selected due to its role as a different therapy to complement the functional mechanism mediated by DOX, BLEO, and MTX. It was also chosen to demonstrate the reconcile nature of the FSC platform and its ability to deliver a combination of both unmodified and ND-modified drugs. In addition, NDs serve as an ideal drug delivery candidate for rapid ND-drug synthesis, increased retention time, improved drug safety, and drug tolerance in tissues.

4.2 Control Cell Lines and Cancer Cell Lines

General chemotherapy agents may cause side effects due to their toxicity in other tissues and cause their limitation in cancer therapy[38-40], such as lung and heart. Drug resistance is another well-known factor that restricts therapeutic efficiency in cancer therapy. It even varies in different types cancer cells of the same tissue. The common reason for acquisition of resistance to a broad range of anticancer drugs is the expression of APT-dependent transporters that detect and eject anticancer drugs from cells. Moreover, Drug resistance contributes to treatment failure in more than 90% of metastatic cancers. Thus, methods to overcome drug resistance and drug toxicity would significantly improve cancer survival rates[41,42]. To show that the FSC-based ND-combination therapy could lower the toxicity in the physiological environment and eliminate drug resistance, three different kinds of control cell lines and three types of breast cancer cell

lines with varying resistance were chosen and compared. The human breast epithelial cell, MCF10A, the human lung fibroblast, IMR-90, and rat myocardium, H9C2 were chosen as control cell lines to demonstrate the safety of the FSC-optimized ND-drug combinations in the preclinical stage. As for the characteristics in these cancer cell lines, MDA-MB-231 is a cancer cell in the breast gland and expresses both EGF and TGF-α receptors. The MDA-MB-231 shows a high resistance level in anticancer drugs[43]. Both BT20 and MCF7 are TGF-β sensitive breast cancer cell lines but are derived from a different part of the breast[44]. Based on the results from the FSC-optimized ND-drug combination, single drug administration, unmodified drug combination, and randomly sampled ND-drug combination (Figure 5, 7, 8, Table 2), it is clear that FSC-optimized ND-drug combination provides a safe and more efficient platform in cancer treatment. It generally shows better therapeutic windows over the other three strategies by being less toxic healthy cells from the lung, breast, and heart while showing good efficacy in combating different drug resistance of breast cancer cells.

4.3 Optimization of ND-Drug Combinations by the Cellular Response and the Therapeutic Windows

In the case of the feedback system control, the therapeutic efficacy algebra series was regarded as a therapeutic window T(c), where T(c) was expressed by:

$$T(c) = V_{fsc}(d,c) - V_{fsc}(d,0) = FSC_{control}(c) - FSC_{cancer}(c)$$

Where $FSC_{control}(c)$ and $FSC_{cancer}(c)$ were defined as the viability of the control cell lines and the cancer cell lines in the FSC platform system. Due to synergism and antagonism of the interaction

in various concentrations and types of drugs, the therapeutic window was represented by a multidimensional response surface. The optimal combination of the drugs characterized by a maximum therapeutic window was found on this response surface. Although the value of $V_{fsc}(d,c)$ and $V_{fsc}(d,0)$ are unknown, their difference can be derived from the result of the experiments. That is, the therapeutic efficacy can be determined and consider varying drug resistant properties of cancer cells without investigating complex intracellular mechanisms and iterative high-throughput screenings.

4.4 Drug Combinations from the Feedback System Control Platform Show Better Therapeutic Optimization than the group of Single Drug Administration

Even conjugated with nanoparticles, the therapeutic efficacy of single drugs could be suboptimal as a result of cancer cell's ability in adapting to unfavorable environment quickly and finding an alternative mechanism to survive. The remedial efficiency of unmodified single drug could be far more suboptimal. Using combinatorial nanomedicines is regarded as an ideal solution to overcome drug resistance and improve therapeutic effects. Therefore, to prove that the FSC-based ND-drug combinations demonstrate better curative effects than single anticancer drug optimization, including unmodified doxorubicin, bleomycin, mitoxantrone, paclitaxel, ND-DOX, ND-BLEO, and ND-MTX. The therapeutic windows between two systems were compared. In the case of MCF10A – MDA-MB-231 (Figure 5), the therapeutic window derived from the FSC-optimized ND-drug combination was 51.50±3.51%, while the optimal therapeutic window generated from the optimal single drug administration was 30.22±10.62% in the use of ND-BLEO. As a result, the FSC-optimized ND combination exceeded the optimal single drug

mediation by 21.28%. In the case of IMR-90−BT20 and IMR-90−MCF7, the optimal therapeutic windows derived from the group of FSC-based ND-drug combinations also showed better performance than either the group of unmodified single drug or single ND-drug (Figure 6G, H). DOX, MTX, BLEO, and ND-MTX had therapeutic windows of less than 10%, barely showing a major therapeutic effect. Also, it should be noticed that the main effector anticancer drug in the FSC-optimized ND-drug combination was ND-MTX instead of ND-BLEO (Figure 5). Thereby it showed that the ND-drug combinations could change the main effector drug and thus varying medicating effects from the single drugs. This phenomenon may result from the interactions between anticancer drugs and may contribute to a different drug efficacy in multi-drug treatments[45-77]. However, in the case of MCF10A−BT20, MCF10A−MCF7, H9C2−MDA-MB-231, H9C2−BT20, H9C2−MCF7, IMR-90−MDA-MB-231, the FSC-based ND-drug combinations failed to better perform in either the group of unmodified or ND-modified single anticancer drugs in maximizing the therapeutic windows (Figure 6). Failure to significantly increase efficiency in eliminating cancer cells while keeping the control cells alive may be due to an antagonistic interaction between drugs in the ND-drug combinations in particular intracellular environments [48,49].

4.5 Drug Combinations from the Feedback System Control Platform Shows Better Therapeutic Optimization than the group of FSC-based Unmodified Drug Combinations

Therapeutic agents that composed several anticancer drugs targeting to different pathways in tumor cells are widely use in chemotherapy, yet their remedial effects are still limited due to side effects and drug resistance. The advantages of the FSC-based ND-drug system lies in its rapid and accurate prediction from phenotypically response and produce optimal drug combinations

according to types of diseased organisms as well as enhance drug efficacy. To show that our FSC-based ND-drug system can better therapeutic effects than the unmodified drug combinations, a comparative study between the FSC-based ND-drug combinations and FSC-based unmodified-drug combinations was conducted. The null hypothesis was that the difference between the two therapeutic windows was normally distributed, with mean as zero and unknown variance. A paired sample t-test was conducted to compare two population mean. If a p-value is smaller than 0.05, the null hypothesis will be rejected, the difference of the mean is not equals to zero, indicating that there is significant difference between the therapeutic windows derived from the two groups. In the pair of MCF10A−MDA-MB-231, the therapeutic windows of the optimal ND-drug combination and unmodified-drug combination were 51.50 ±3.51% and 31.10 ±2.50%, respectively. Therefore, even derived from the FSC platform, the optimal unmodified-drug combinations was lower than the optimal FSC ND-drug combinations in the therapeutic window by 20.40%, with a p-value of 0.0146 (Figure 7A). In the group of H9C2−MDA-MB-231, the optimal therapeutic window of the FSC ND-drug combinations was 21.46±4.00%, while the optimal one from the FSC-based unmodified-drug combinations was 4.94±5.06%. Therefore, the optimal FSC ND-drug combinations outperformed the optimal FSC unmodified combinations in the therapeutic window by 16.52%, with 0.0012 as a p-value (Figure 7B). In the pair of IMR-90−MDA-MB-231, the therapeutic windows for the optimal FSC-based ND-drug combination and FSC-based unmodified-drug combination were 15.80±6.19% and 2.20±3.66%, respectively. Based on this experimental outcome, given the same feedback system control platform, the optimal ND-drug combination outperformed the optimal unmodified-drug combination by 13.6%, with a p-value of 0.0301 (Figure 7C).

In addition, from the comparisons between the optimal FSC-based ND-drug combination and the optimal FSC-based unmodified-drug combination in the three cases mentioned above, it is clear that the FSC-derived ND-drug combinations incorporated different drug dosages toward the mediating of improved therapeutic windows. Therefore, with the advantages of the ND-drugs, which have shown the ability to overcome the issues in drug resistance and increase retention time in tumors, it is reasonable to assume that the FSC-based ND-drug combination serves as a better candidate in improving therapeutic efficacy over the FSC-based unmodified-drug combination method.

4.6 Drug Combinations from the Feedback System Control Platform Shows Better Therapeutic Optimization than the group of Randomly Sampled ND-Drug Combinations

Although the ND-drug combination has advantages in lowering cellular toxicity, enhancing intra-tumor retention time, and improving therapeutic efficacy, the ratio of each drug in drug combinations also plays an important role in drug efficacy. The ideal combinatorial therapeutic effects may require specific ratio of each curative agents. The randomized ratio of drug levels may result in limited treatment effects[50]. To show that the ideal drug combinations considering varying diseased profiles can be achieved by the feedback system control methodology, the ND-drug combinations were randomly sampled and compared with the one generated from the FSC platform. From Table 3 and Figure 8, we can conclude that the randomized ND-drug combinations lead to insignificant effects in maximizing the therapeutic window. In the pair of H9C2−MCF7, the optimal therapeutic window generated from the FSC-optimized ND-drug combinations surpassed the average randomized combinations by 42.66% (p-value= 6.39×10^{-4},

Table 3). While in the pair of MCF10A−MDA-MB-231, the most extreme case, the optimal therapeutic window generated from FSC ND-drug combination exceeded the one in randomized ND-drug combination by 62.43% (p-value=9.39×10^{-18}, Table 3). Moreover, only 22.8% of the randomized combination samples (two out of nine) showed the positive therapeutic windows. As a result, based on the assumption that a random sampling method samples the space uniformly, the probability of finding a ND-drug or unmodified drug combination with a positive therapeutic window is difficult. Thus, the inherent FSC platform is preferable in converging toward a global optimal combination and provides a better strategy in combating cancers.

4.7 The Robustness and the Application of ND-Drug Combinations through the Feedback System Control Optimization

Based on the previous studies and the experimental results of this study, it is clear that with the mediation of NDs, the safety and therapeutic efficacy can be greatly improved compared to unmodified single drug medication, which serves as a clinical standard of treatment for several cancers. On the other hand, the traditional way to obtain the optimal drug combinations is by using high-throughput screening. The ideal combinations of the chemotherapeutic agents are determined through repeatedly testing and validation. This method turns out to be insufficient because the possible number of drug combinations increases exponentially with each increase in the number of new drugs and its application in clinical treatment is highly challenging. The FSC platform, instead, has demonstrated a unique advantage in optimizing drug combinations by producing the complete response surface with few numbers of experiments and rapidly produces optimal drug combinations. It does not require complex cellular signaling pathways and theoretical assumptions for model prediction. For the current clinical stage, either unmodified

single drug administration or drug combinations serve as a standard treatment in chemotherapy. It is well known that drug resistance and drug toxicity lead to limited therapeutic efficacy and remain a major challenge in cancer therapeutic improvement. Therefore, with the association of ND-drugs and the FSC platform, such strategy can be very promising in improving therapeutic effects against cancers. ND-drugs serve as mediators that could highly reduce drug toxicity and drug resistance, and increases drug safety as well as therapeutic efficacy. Also, it is able to construct a response graph to specifically point out the optimal drug combinations with optimized curative effects and safeness. The FSC-based ND-drug platform systemically addresses the issue in drug resistance. The cancer cell lines used in this study were shown to have different drug resistances. The combinations of the drugs in the FSC platform could be removed or replaced by new candidates according to types of cancers. The FSC platform can also be feasible to an extensive range of other drugs or chemical compounds. The FSC platform can swiftly converge to the global optimal dosages and combinations accounting for varying drug resistance, therefore showing the ability to respond against tumor cells' dynamics against drugs. In addition to *in vitro* studies, a curative way that composed the FSC platform with nanomedicine combinations is believed as a novel and an efficient way in combating cancers.

4.8 Limitations and Future Directions

Based on the direct phenotypic response from the input stimuli, the feedback system control methodology has showed a strong and efficient ability in optimizing drug combinations for desire cellular activities. It can be widely adapted to various kinds of therapeutic agents and utilized in other biological applications[51,52]. Yet, its efficacy has been only achieved in *in intro*

and preclinical stage, which only consider at the individual level that often used as experimental models instead of studying complicated physiological environment in human beings. In the clinic, deriving preferable phenotypic response, which is highly to be conducted at the level of tissues, organs, or functional systems, seems to be much more complex and challenging. A time period of acquiring phenotypic response might be longer compared to *in vitro* studies. However, to circumvent such uncertainties and difficulties faced in developing a mature feedback system control platform that can be used clinically, more algorithms of sampling and optimization beyond cellular level as well as other organism models should be further tested and studied.

5. Conclusions

In summary, traditional single drug and combinatorial drug therapies have faced great obstacles in cancer treatment due to drug resistance and safety issues. To solve these problems, a method that associates the FSC platform with ND-drugs has been introduced. FSC can rapidly construct a response surface according to the experimental data. It produces the global optimal dosages and combinations within a small number of experiments without iterative screening. ND-drugs can greatly lower the resistance and toxicity of the drug, and thereby improve drug efficacy as well as safety. The FSC-optimized ND-drug combinations show better therapeutic effects than ones in the single drug administration, unmodified drug combinations and randomly sampled ND-drug combinations. This approach provides a robust and flexible system design in drug combinations efficiently. Although there are still researches to be done to prove its feasibility in clinical use, it shows great potential in becoming a new strategy to fight cancers and is highly applicable in realizing personalized medication in the future.

Figures and Tables

name	max concentration [M]	fold
ND-DOX	9.00E-05	4.50
ND-BLEO	2.00E-06	4.47
ND-MTX	1.30E-04	6.18
PAC	2.00E-05	6.80

Table 1. Maximum concentration of ND-drugs in the combinations and folds of seven serial dilution stages. The maximum concentration was determined based on the cellular viability (n=3). The concentration range of each drug was sectioned into seven dilution stages with the different fold. It was 4.5 folds for ND-DOX, 4.47 folds for ND-BLEO, 6.18 folds for ND-MTX, and 6.8 folds for paclitaxel.

	[level]			
#	ND+Dox	ND+Bleo	ND+MTX	paclitaxel
1	3	1	4	1
2	4	2	5	3
3	2	3	5	4
4	1	5	5	5
5	4	6	3	7
6	7	3	5	5
7	2	7	3	3
8	2	1	6	7
9	2	5	1	6
10	2	4	6	4
11	5	7	2	5
12	4	6	5	4
13	4	2	3	7
14	5	3	4	3
15	6	2	2	6
16	2	3	3	6
17	3	3	5	3
18	1	3	7	5
19	2	6	6	7
20	1	4	4	6
21	2	5	7	2
22	6	4	4	1
23	6	5	5	4
24	4	2	6	1
25	6	5	2	2
26	3	3	1	1
27	4	1	6	5
28	3	6	3	2
29	5	6	5	7
30	7	2	7	5
31	3	4	2	6
32	5	5	2	3
33	4	2	4	3
34	5	1	4	5
35	6	3	4	6
36	3	2	4	6
37	7	6	2	6
38	1	6	3	6

39	4	6	3	4
40	6	7	1	4
41	2	4	2	2
42	3	5	7	4
43	3	3	6	5
44	4	2	5	2
45	6	3	1	3
46	3	4	4	3
47	5	4	1	4
48	7	5	4	4
49	6	4	6	3
50	6	6	6	1
51	7	4	2	3
52	2	6	2	2
53	5	2	5	5
54	5	5	3	5
55	6	7	3	2
56	5	2	6	2
57	3	6	7	2

Table 2. Latin hypercube sampling in ND-drug combinations. A total of 57 combinations were produced based on Latin hypercube sampling. The serial dilution range of each drug was divided into seven stages. Each number represents the stage number.

	Cell pairs	H9C2-BT20	H9C2-MCF-7	H9C2-MDA0MB-231	IMR-90-BT20	IMR-90-MCF7	IMR-90-MDA-MB-231
[%]	OPT TW	0.27	0.22	0.21	0.25	0.11	0.16
	STD	0.08	0.08	0.04	0.04	0.06	0.06
	AVG TW	0.03	-0.20	-0.02	0.02	-0.21	-0.04
	AVG STD	0.07	0.09	0.07	0.08	0.09	0.07
concentration	ND-DOX	9.88E-07	4.88E-08	4.88E-08	2.19E-07	9.88E-07	1.08E-08
	ND-BLEO	1.12E-09	2.00E-06	2.00E-06	2.24E-08	1.12E-09	4.47E-07
	ND-MTX	3.41E-06	8.93E-08	2.34E-09	1.45E-08	5.52E-07	8.93E-08
	PAC	9.35E-09	9.35E-09	2.00E-05	2.94E-06	9.35E-09	2.94E-06
	p-value	3.99E-02	6.39E-04	4.96E-03	1.35E-02	4.89E-03	4.53E-02

	Cell pairs	MCF10A-BT20	MCF10A-MCF7	MCF10A-MDA0MB-231
[%]	OPT TW	0.50	-0.04	0.52
	STD	0.04	0.06	0.04
	AVG TW	-0.05	-0.29	-0.11
	AVG STD	0.07	0.08	0.06
concentration	ND-DOX	9.88E-07	9.88E-07	9.88E-07
	ND-BLEO	1.12E-09	1.12E-09	1.12E-09
	ND-MTX	2.10E-05	2.10E-05	2.10E-05
	PAC	2.02E-10	2.02E-10	2.02E-10
	p-value	1.51E-12	2.11E-02	9.39E-18

Table 3. The FSC-optimized therapeutic windows versus the average therapeutic windows.

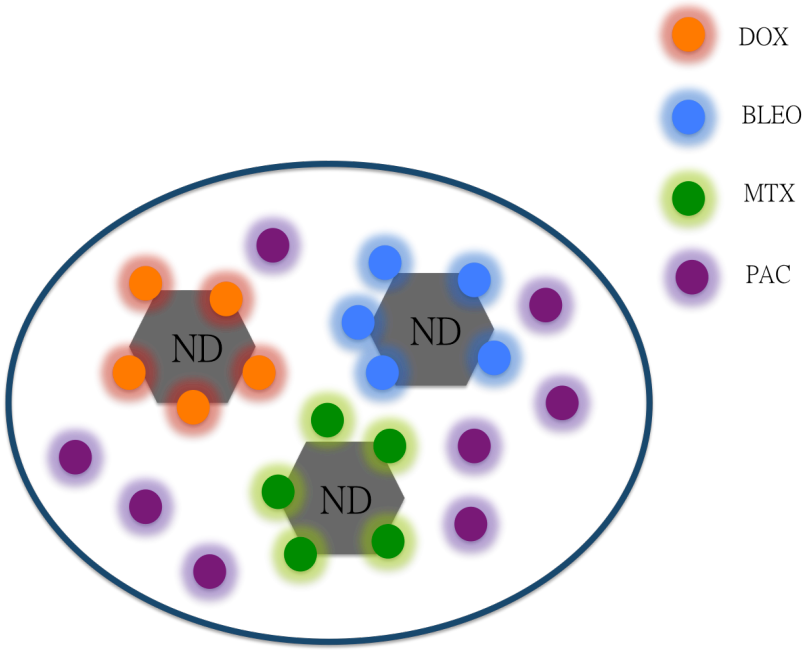

Figure 1. Overview of the combinatorial drugs for the FSC platform. The combinatorial drug used by the FSC platform is consists of four various kinds of drug: Nanodiamond-doxorubicin (ND-DOX), nanodiamond-bleomycin (ND-BLEO), nanodiamond-mitoxantrone (ND-MTX), and paclitaxel (PAC).

STEP 1:

- Determination of concentration in each drug through viability test.
- Use Latin hypercube sampling to generate 57 combinations.

STEP 2:

- Response surfaces are created through analyzing the viability in the both cancer cell lines and control cell lines.
- Constructions of the therapeutic windows.

STEP 3:

- Derive the optimal combination on the surface of the therapeutic windows by the differential evolution approach.

Figure 2. The flow of the FSC platform.

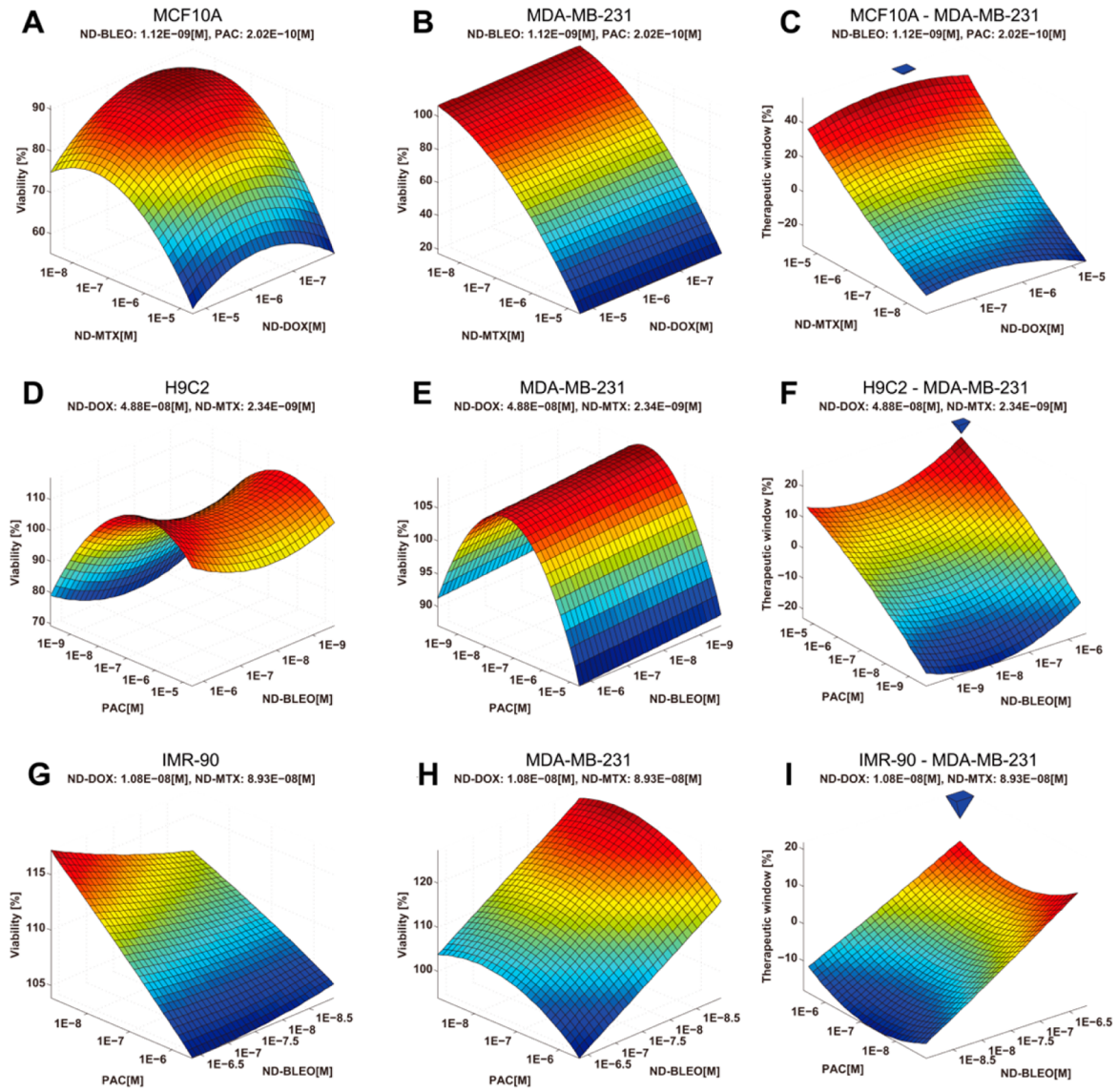

Figure 3. Formation of the cellular response surfaces and therapeutic window surfaces. (A),(B),(D),(E),(G),(H) Six five-dimensional cellular surfaces (n=3 in each case) were constructed in both control cell line and cancer cell line by fixing two drug concentrations as an anchor point. The surface was plotted by MATLAB by varying the concentration of the two other drugs according to cell viability. (C),(F),(I) Three therapeutic window surfaces (n=3 in each case) were plotted based on the result of the cellular response surface. The differential evolution optimization was utilized to locate global optimal dosage on the therapeutic window

surface (deep red).

*therapeutic window = viability of control cell line - viability of cancer cell line.

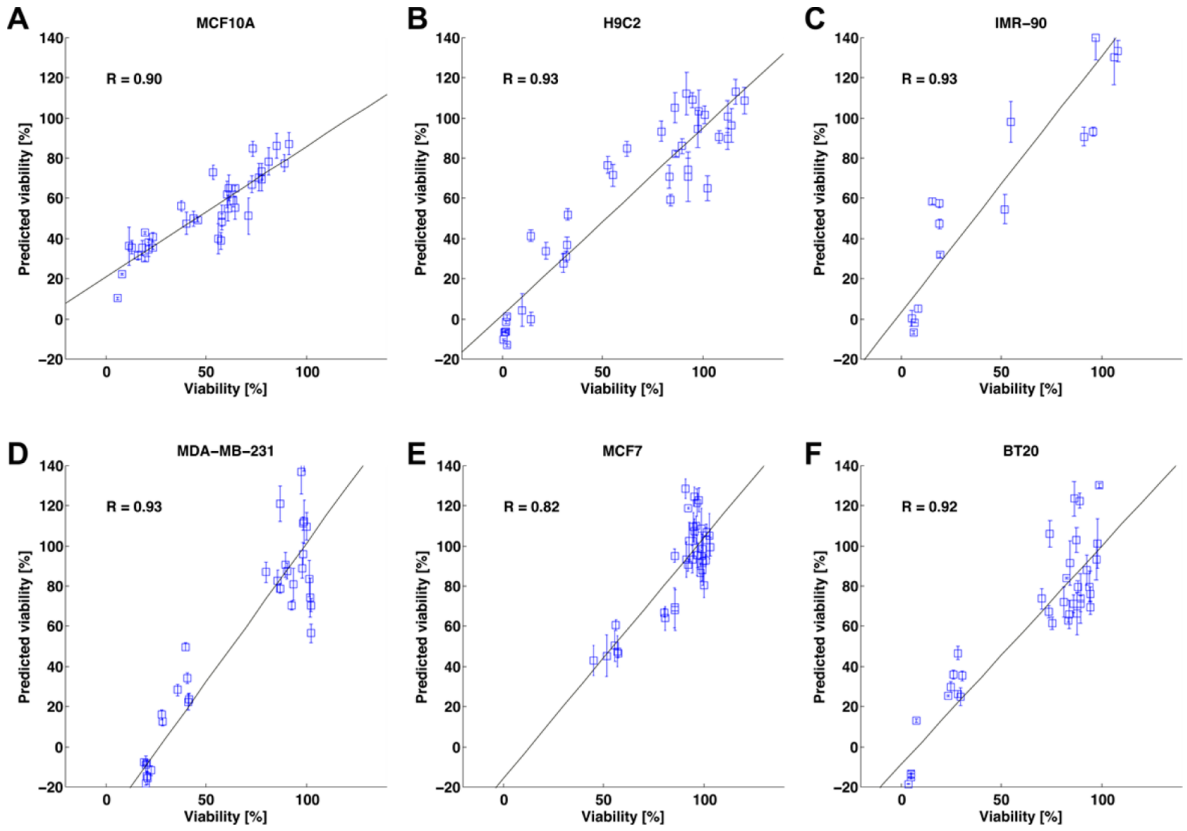

Figure 4. Pearson correlation plots for verification of experimental results with the FSC model predictions. Pearson correlation plots of the FSC-predicted viabilities versus experimental data of three control cell lines and three cancer cell lines in the verifications (A) MCF10A, r=0.9 (B) H9C2, r=0.93 (C) IMR-90, r=0.93 (D) MDA-MB-231, r=0.93 (E) MCF7, r=0.82 and (F) BT20, r=0.92 (n=3).

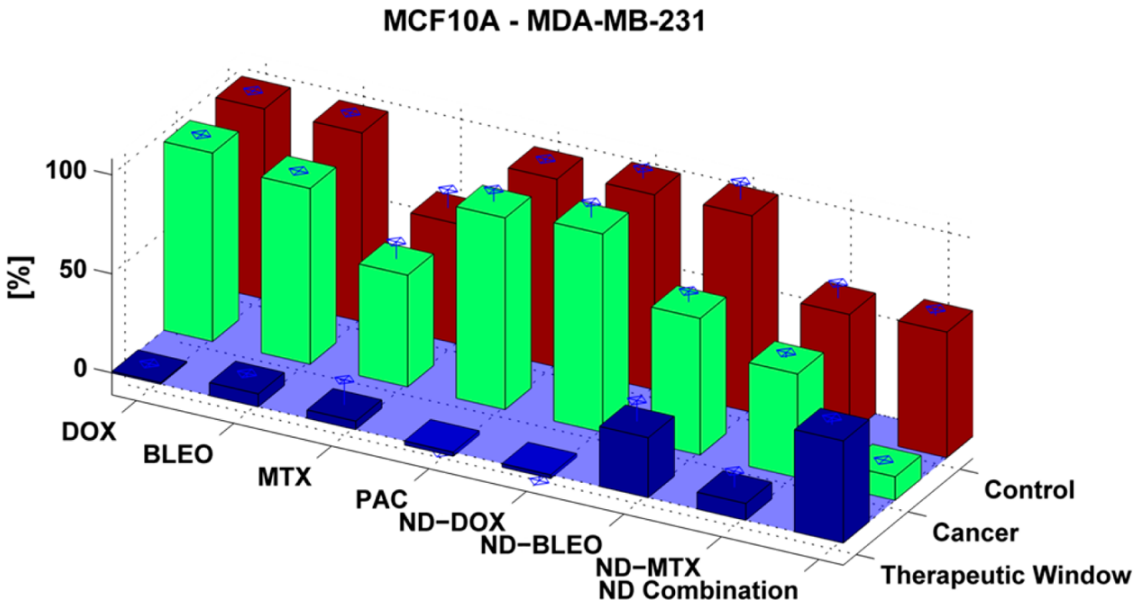

single drug	DOX	BLEO	MTX	PAC	ND-DOX	ND-BLEO	ND-MTX
[M]	7.63E-10	7.63E-10	1.25E-05	7.63E-10	7.63E-10	1.95E-07	5.00E-05

combination	ND-DOX	ND-BLEO	ND-MTX	PAC
[M]	9.88E-07	1.12E-09	2.10E-05	2.02E-10

Figure 5. The FSC-based ND-drug combination performance v.s the single ND-drug and unmodified drug administration in MCF10A and MDA-MB-231 cell lines. Red bar represents the viability of the control cell line, MCF10A, while the light green bar graph demonstrates the viability of the cancer cell line, MDA-MB-231. The blue bar indicates the therapeutic window, MCF10A−MDA-MB-231. Each drug or drug combination in the experiment was an optimal dosage (n = 3). The standard error is represented by length of the vertical blue line on the top of the bar. The optimal drug concentration for each scenario is shown at the bottom.

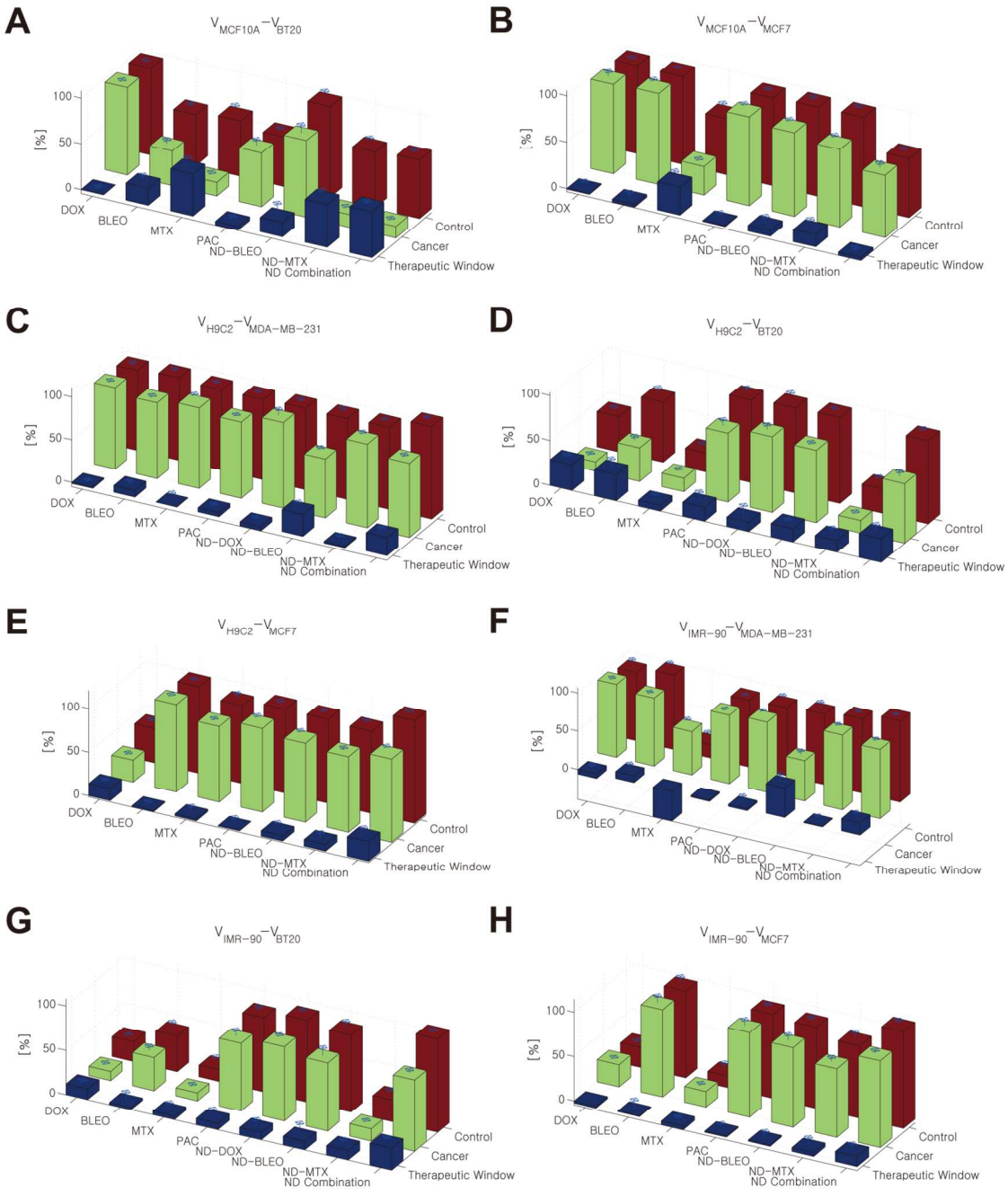

Figure 6. The therapeutic window of the FSC-optimized ND-drug combinations versus the optimal single drug administration in the rest cell lines. Bar graph showing the therapeutic window between the viabilities of the cancer cells, MDA-MB-231, MCF7, BT20 and control cells, MCF10A, H9C2, and IMR-90 from the optimal concentration of each drug or ND-drug

combination in the experiment (n=3). The length of the vertical blue line indicates the standard error of each condition.

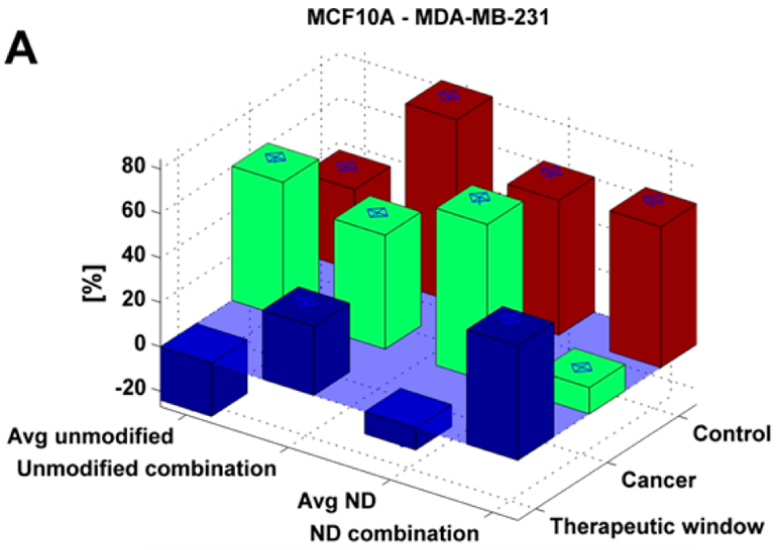

[M]	ND-DOX	ND-BLEO	ND-MTX	PAC
Unmodified	1.08E-08	2.50E-10	3.41E-06	9.35E-09
ND	9.88E-07	1.12E-09	2.10E-05	2.02E-10

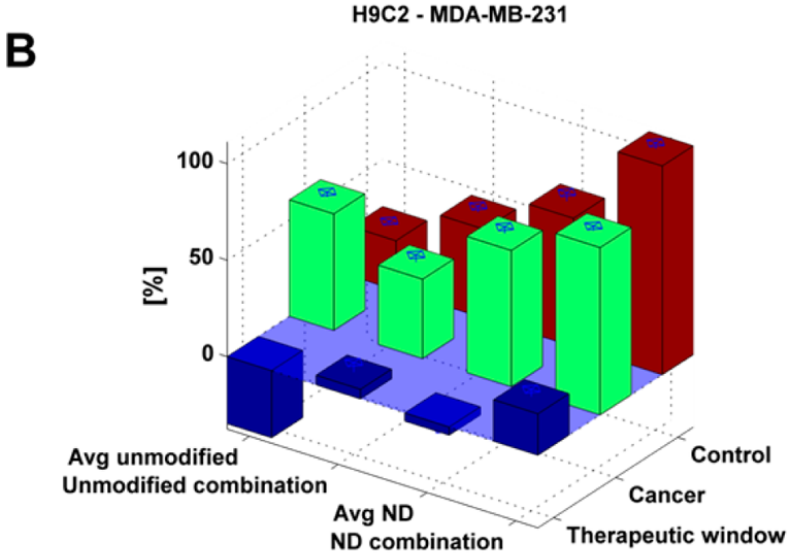

[M]	ND-DOX	ND-BLEO	ND-MTX	PAC
Unmodified	9.00E-05	1.00E-07	2.34E-09	2.02E-10
ND	4.88E-08	2.00E-06	2.34E-09	2.00E-05

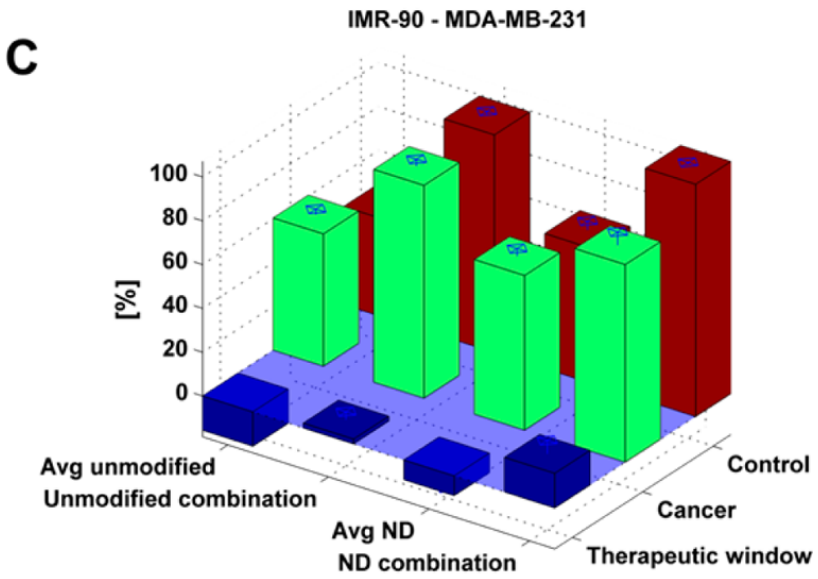

[M]	ND-DOX	ND-BLEO	ND-MTX	PAC
Unmodified	1.08E-08	2.50E-10	2.34E-09	2.02E-10
ND	1.08E-08	4.47E-07	8.93E-08	2.94E-06

Figure 7. Comparison of the therapeutic window between the FCS-optimized ND-drug combinations and the unmodified drug combinations. The therapeutic windows were conducted in the ND-combination and the unmodified combination in three pairs of control-cancer cells: MCF10A v.s MDA-MB-231, H9C2 v.s MDA-MB-231, and IMR-90 v.s MDA-MB-231 (n=3). The optimal drug concentrations are shown in the table at the bottom of the graph.

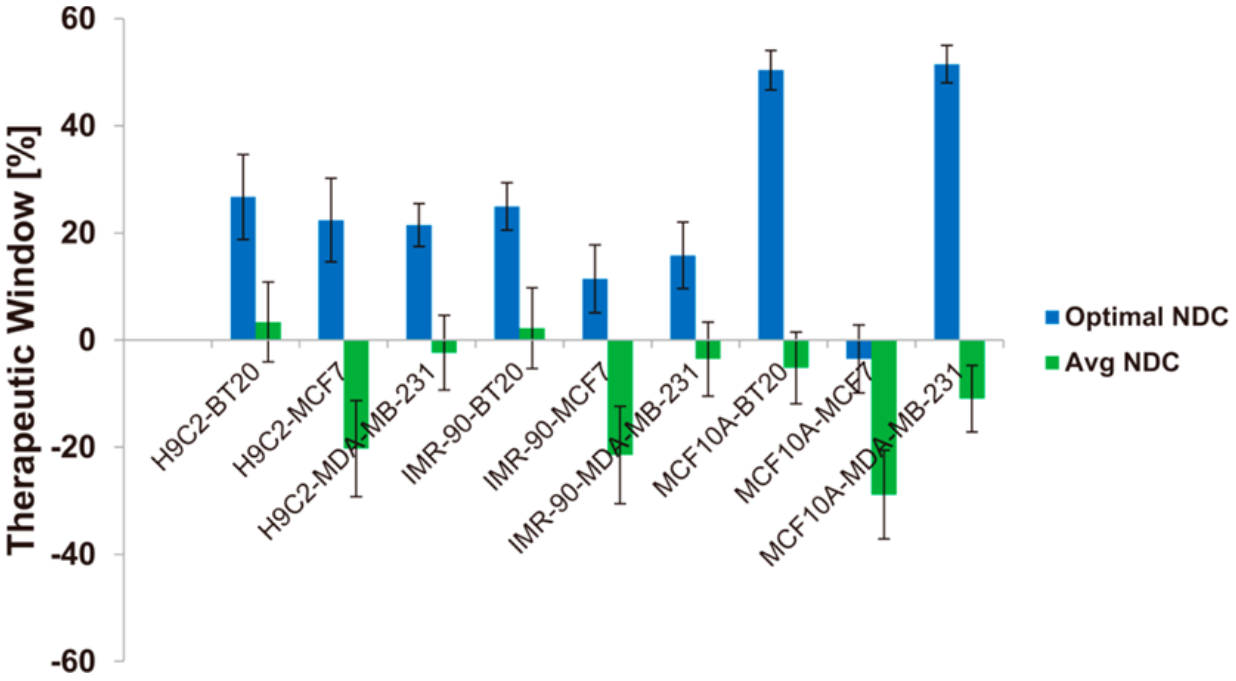

Figure 8. The therapeutic window of FSC-optimized ND-drug combination versus randomized ND-drug combinations. The therapeutic windows between each control cell line and each cancer cell line are shown. Cancer cell lines include MDA-MB-231, MCF7, and BT20 and control cell lines include MCF10A, H9C2, and IMR-90, forming a total of nine possible cancer-control cell line pairs (n = 3).

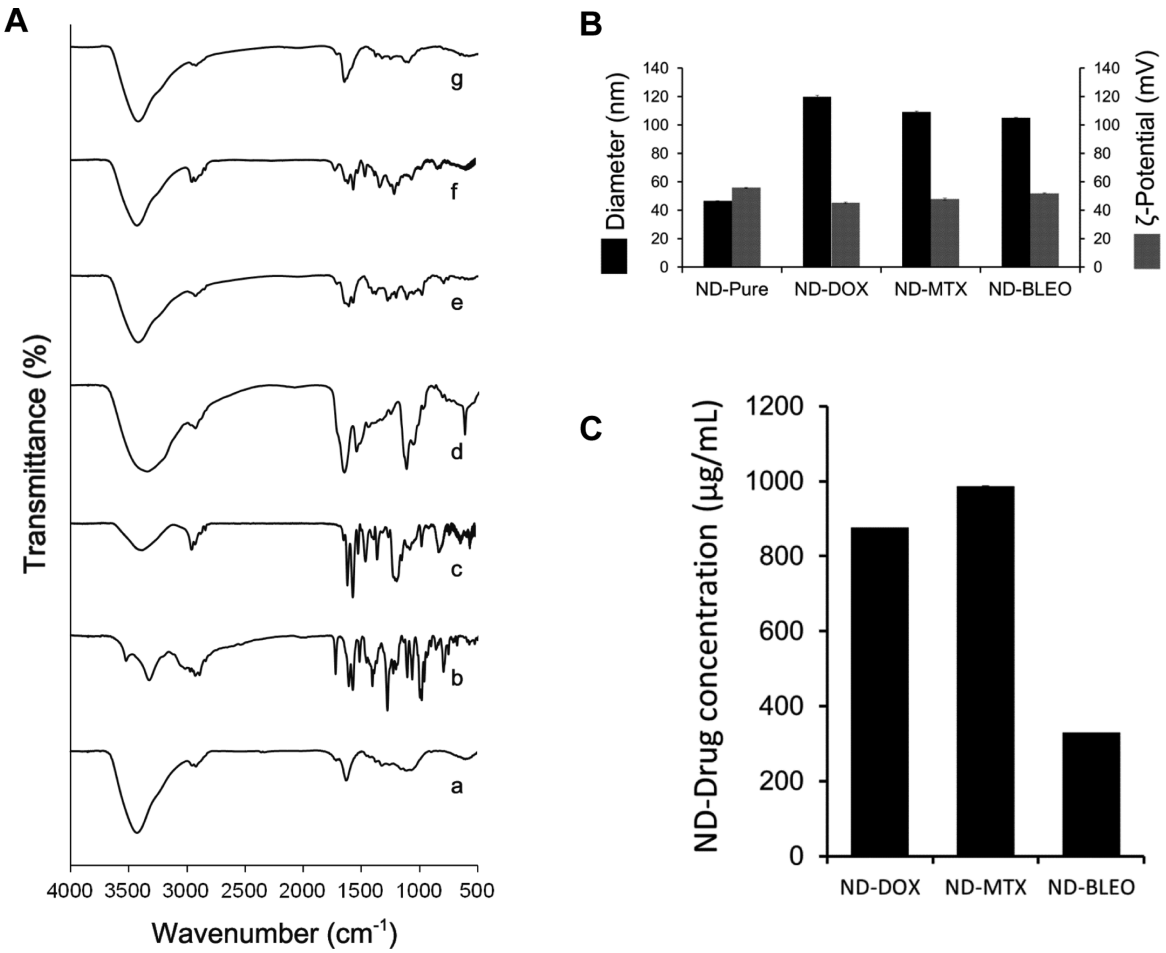

Figure 9. Synthesis and characterization of ND-drugs. (A) FTIR spectra of (a) NDs, (b) doxorubicin (DOX), (c) mitoxantrone (MTX), (d) bleomycin (BLEO), (e) ND-DOX, (f) ND-MTX, and (g) ND-BLEO. (B) Sizes of the ND and ND-drugs analysis by dynamic light scattering. The picture indicated the diameters (n=5) of NDs and ND-drugs and their ζ-potentials (n=3). (C) Drug concentrations of DOX, MTX, and BLEO in each 1 mL of ND-drug solution (n = 3).

References

1. Kang, Byoung Heon, et al. "Combinatorial drug design targeting multiple cancer signaling networks controlled by mitochondrial Hsp90." The Journal of clinical investigation 119.3 (2009): 454.

2. Cole, S. P. C., et al. "Overexpression of a transporter gene in a multidrug-resistant human lung cancer cell line." SCIENCE-NEW YORK THEN WASHINGTON- 258 (1992): 1650-1650.

3. Gottesman, Michael M., Tito Fojo, and Susan E. Bates. "Multidrug resistance in cancer: role of ATP–dependent transporters." Nature Reviews Cancer 2.1 (2002): 48-58.

4. Doyle, L. Austin, et al. "A multidrug resistance transporter from human MCF-7 breast cancer cells." Proceedings of the National Academy of Sciences 95.26 (1998): 15665-15670.

5. Bodley, Annette, et al. "DNA topoisomerase II-mediated interaction of doxorubicin and daunorubicin congeners with DNA." *Cancer research* 49.21 (1989): 5969-5978.

6. Nitiss, John L. "Targeting DNA topoisomerase II in cancer chemotherapy."*Nature Reviews Cancer* 9.5 (2009): 338-350.

7. Baselga, Jose, et al. "Recombinant humanized anti-HER2 antibody (Herceptin™) enhances the antitumor activity of paclitaxel and doxorubicin against HER2/neu overexpressing human breast cancer xenografts." *Cancer research* 58.13 (1998): 2825-2831.

8. Sledge, George W., et al. "Phase III trial of doxorubicin, paclitaxel, and the combination of doxorubicin and paclitaxel as front-line chemotherapy for metastatic breast cancer: an intergroup trial (E1193)." *Journal of Clinical Oncology* 21.4 (2003): 588-592.

9. Swain, Sandra M., Fredrick S. Whaley, and Michael S. Ewer. "Congestive heart failure in patients treated with doxorubicin." *Cancer* 97.11 (2003): 2869-2879.

10. Hay, John, Shahriar Shahzeidi, and Geoffrey Laurent. "Mechanisms of bleomycin-induced lung damage." *Archives of toxicology* 65.2 (1991): 81-94.

11. Stuart-Harris, Robin C., et al. "Mitoxantrone: an active new agent in the treatment of advanced breast cancer." *Cancer chemotherapy and pharmacology* 12.1 (1984): 1-4.

12. Tannock, Ian F., et al. "Docetaxel plus prednisone or mitoxantrone plus prednisone for advanced prostate cancer." *New England Journal of Medicine*351.15 (2004): 1502-1512.

13. Sledge Jr, G. W., et al. "Paclitaxel (Taxol)/doxorubicin combinations in advanced breast cancer: the Eastern Cooperative Oncology Group experience."*Seminars in oncology*. Vol. 21. No. 5 Suppl 8. 1994.

14. Al-Lazikani, Bissan, Udai Banerji, and Paul Workman. "Combinatorial drug therapy for cancer in the post-genomic era." Nature biotechnology 30.7 (2012): 679-692.

15. Fitzgerald, Jonathan B., et al. "Systems biology and combination therapy in the quest for clinical efficacy." Nature chemical biology 2.9 (2006): 458-466.

16. Giordano, S., and A. Petrelli. "From single-to multi-target drugs in cancer therapy: when aspecificity becomes an advantage." Current medicinal chemistry 15.5 (2008): 422-432.

17. Pritchard, Kathleen I., et al. "HER2 and responsiveness of breast cancer to adjuvant chemotherapy." New England Journal of Medicine 354.20 (2006): 2103-2111.

18. Mann, John. "Natural products in cancer chemotherapy: past, present and future." Nature Reviews Cancer 2.2 (2002): 143-148.

19. Chabner, Bruce A., and Thomas G. Roberts. "Chemotherapy and the war on cancer." Nature Reviews Cancer 5.1 (2005): 65-72.

20. Komarova, Natalia L., and C. Richard Boland. "Cancer: calculated treatment."Nature 499.7458 (2013): 291-292.

21. Kareva, Irina, David J. Waxman, and Giannoula Lakka Klement. "Metronomic chemotherapy: An attractive alternative to maximum tolerated dose therapy that can activate anti-tumor immunity and minimize therapeutic resistance." Cancer letters 358.2 (2015): 100-106.

22. Tallarida, Ronald J. "An overview of drug combination analysis with isobolograms." Journal of Pharmacology and Experimental Therapeutics 319.1 (2006): 1-7.

23. Collins, Jerry M., et al. "Nonlinear pharmacokinetic models for 5‐fluorouracil in man: Intravenous and intraperitoneal routes." Clinical Pharmacology & Therapeutics 28.2 (1980): 235-246.

24. Tallarida, Ronald J. "Drug synergism: its detection and applications." Journal of Pharmacology and Experimental Therapeutics 298.3 (2001): 865-872.

25. Al-Shyoukh, Ibrahim, et al. "Systematic quantitative characterization of cellular responses induced by multiple signals." *BMC systems biology* 5.1 (2011): 88.

26. Gaitanis, Alexander, and Stephen Staal. "Liposomal doxorubicin and nab-paclitaxel: nanoparticle cancer chemotherapy in current clinical use." Cancer Nanotechnology. Humana Press, 2010. 385-392.

27. Davis, Mark E., and Dong M. Shin. "Nanoparticle therapeutics: an emerging treatment modality for cancer." Nature reviews Drug discovery 7.9 (2008): 771-782.

28. Brannon-Peppas, Lisa, and James O. Blanchette. "Nanoparticle and targeted systems for

cancer therapy." Advanced drug delivery reviews 64 (2012): 206-212.
29. Adnan, Ashfaq, et al. "Atomistic simulation and measurement of pH dependent cancer therapeutic interactions with nanodiamond carrier." Molecular pharmaceutics 8.2 (2011): 368-374.

30. Chow, Edward K., et al. "Nanodiamond therapeutic delivery agents mediate enhanced chemoresistant tumor treatment." Science translational medicine3.73 (2011): 73ra21-73ra21.

31. El-Say, Khalid Mohamed. "Nanodiamond as a drug delivery system: Applications and prospective." (2011).

32. Moore, Laura K., et al. "Diamond-based nanomedicine: Enhanced drug delivery and imaging." Disruptive Science and Technology 1.1 (2012): 54-61.

33. Torre, V., and T. Poggio. "A synaptic mechanism possibly underlying directional selectivity to motion." Proceedings of the Royal Society of London B: Biological Sciences 202.1148 (1978): 409-416.

34. Risken, Hannes. Fokker-Planck Equation. Springer Berlin Heidelberg, 1984.

35. Lande, Russell, and Stevan J. Arnold. "The measurement of selection on correlated characters." Evolution (1983): 1210-1226.

36. Neuberger, Tobias, et al. "Superparamagnetic nanoparticles for biomedical applications: possibilities and limitations of a new drug delivery system." *Journal of Magnetism and Magnetic Materials* 293.1 (2005): 483-496.

37. Nagarwal, Ramesh C., et al. "Polymeric nanoparticulate system: a potential approach for ocular drug delivery." *Journal of Controlled Release* 136.1 (2009): 2-13.

38. Lindley, Celeste, et al. "Perception of chemotherapy side effects cancer versus noncancer patients." Cancer practice 7.2 (1999): 59-65.

39. Ratajczak, Mariusz Z., et al. "Induction of a tumor-metastasis-receptive microenvironment as an unwanted and underestimated side effect of treatment by chemotherapy or radiotherapy." Journal of ovarian research 6.1 (2013): 1-10.

40. Sanchez-Barcelo, Emilio J., et al. "Melatonin uses in oncology: breast cancer prevention and reduction of the side effects of chemotherapy and radiation." Expert opinion on investigational drugs 21.6 (2012): 819-831.

41. Gottesman, Michael M. "Mechanisms of cancer drug resistance." *Annual review of medicine* 53.1 (2002): 615-627.

42. D. B. Longley, P. G. Johnston, Molecular mechanisms of drug resistance. J. Pathol. **205**, 275–292(2005).

43. Chen, Jiao, et al. "PKD2 mediates multi-drug resistance in breast cancer cells through modulation of P-glycoprotein expression." Cancer letters 300.1 (2011): 48-56.

44. Kalkhoven, Eric, et al. "Resistance to transforming growth factor b and activin due to reduced receptor expression in human breast tumor cell lines." Cell Growth and Differentiation-Publication American Association for Cancer Research 6.9 (1995): 1151-1162.

45. Jia, Jia, et al. "Mechanisms of drug combinations: interaction and network perspectives." Nature reviews Drug discovery 8.2 (2009): 111-128.

46. Zimmermann, Grant R., Joseph Lehar, and Curtis T. Keith. "Multi-target therapeutics: when the whole is greater than the sum of the parts." Drug discovery today 12.1 (2007): 34-42.

47. Csermely, Péter, Vilmos Agoston, and Sandor Pongor. "The efficiency of multi-target drugs: the network approach might help drug design." Trends in pharmacological sciences 26.4 (2005): 178-182.

48. Chou, Ting-Chao, and Paul Talalay. "Quantitative analysis of dose-effect relationships: the combined effects of multiple drugs or enzyme inhibitors."Advances in enzyme regulation 22 (1984): 27-55.

49. Chou, Ting-Chao. "Theoretical basis, experimental design, and computerized simulation of synergism and antagonism in drug combination studies."Pharmacological reviews 58.3 (2006): 621-681.

50. Jain, Rakesh K. "Normalization of tumor vasculature: an emerging concept in antiangiogenic therapy." Science 307.5706 (2005): 58-62.

51. Tsutsui, Hideaki, et al. "An optimized small molecule inhibitor cocktail supports long-term maintenance of human embryonic stem cells." *Nature communications* 2 (2011): 167.

52. Valamehr, Bahram, et al. "Developing defined culture systems for human pluripotent stem cells." *Regenerative medicine* 6.5 (2011): 623-634.